Technical Physics, 2026, Vol. 71, No. 1

06

Radiation tolerance of ATR sensors based on p-InAsSbP/n-InAs double heterostructures irradiated by gamma-rays

© S.A. Karandashev,[1] A.A. Klimov,[1] R.E. Kunkov,[1] V.N. Lomasov,[2] T.S. Lukhmyrina,[1] B.A. Matveev,[1] M.A. Remennyi,[1] E.I. Shabunina,[1] N.M. Shmidt[1]

[1] Ioffe Institute,
194021 St. Petersburg, Russia
[2] Peter the Great Saint-Petersburg Polytechnic University,
195251 St. Petersburg, Russia
e-mail: bmat@iropt3.ioffe.ru

Received February 17, 2025
Revised September 4, 2025
Accepted September 25, 2025

Radiation tolerance tests of multiply attenuated total reflection sensors and their optoelectronic components (light-emitting diodes and photodiodes) based on p-InAsSbP/n-InAs double heterostructures have shown that their main parameters are stable to exposure to gamma radiation at small irradiation doses (≤ 0.1 MGy, ^{60}Co), while at the irradiation doses from ~ 0.2 to ~ 2 MGy we have detected an increase of a dark current and sensor noises with simultaneous reduction of a photodiode photocurrent as well as found a process of partial restoration of these parameters after exposure at 300 K. An analysis of the dependence of the spectral density of low-frequency current noise on the perimeter and area of $p-n$ junctions allowed us to conclude that the determining contribution is made by radiation defects formed at the periphery of mesa diodes during their irradiation with high doses(~ 2 MGy).

Keywords: InAs, light-emitting diodes, photodiodes, optopairs, mid-IR range, radiation tolerance, surface, radiation defects.

DOI: 10.61011/TP.2026.01.62847.22-25

Introduction

Double heterostructures (DHs) with an n-InAs active layers, which were initially used for obtaining stimulated emission in the mid-IR spectral range at low temperatures, are undoubtedly interesting also because it is possible to use them as a base for manufacturing photodiodes (PDs) [1,2] and light-emitting diodes (LEDs) [3] that are designed to operate at room temperature and used in thermophotovoltaic generators [4,5] fast gas analyzers [6–8] and pyrometers [9]. In addition, the said structures can be also used for designing surface-sensitive chemical sensors [10] and for measuring a chemical composition by a method of multiply attenuated total reflection. „ATR method“ or „evanescent wave measurements“) [11].

One of the conditions required for the ATR measurements is a direct optical contact of a solid body or liquid with a sensor's sensitive area on the crystal/waveguide surface. This contact implements interaction (partial absorption) of an evanescent wave that extends into an analyte during internal reflection of radiation at a crystal/studied sample interface. It makes possible to measure and subsequently analyze a degree of attenuation of intensity of the evanescent wave with the least sample preparation or even without it at all. Therefore, the ATR method is promising for remote measurements without direct presence of an operator, for example, when determining an aging degree of plastic parts and cable coatings in zones of nuclear power plants (NPP), which are hardly accessible or totally inaccessible for humans because of an increased intensity of penetrating radiation, for example, the γ-radiation [12,13]. It is assumed that a desired lifetime of the ATR sensors is to exceed a lifetime of an NPP reactor. For example, it is more than 30 years for the WWR-1000 reactor [14].

Radiation tolerance of InAs crystals was studied when they were exposed to protons [15–19], neutrons [14,20,21] and electrons [21,22]. Less attention was paid to studies that included irradiation of InAs with γ-rays. Thus, for example, the study [23] has just stated that it is possible to create the InAs-based Hall sensors for Tokamak facilities, but has not provided data on radiation tolerance of the samples. It is commonly believed that electro-physical properties of the irradiated InAs crystal are invariant to a type of radiation-induced disturbances of a crystal lattice, which are obtained in various irradiation types [22]. But this invariance still does not unambiguously predict long-term operability of the ATR sensor under harsh conditions at least due to the fact that in addition to the InAs-based $p-n$-heterostructures this sensor also includes passive components that are important for implementing evanescent wave method, namely, a waveguide (the „ATR crystal“) and other structure elements.

The literature on the subject of the present study has data neither on degradation of electrical properties of the InAs-based $p-n$-structures, nor on their noise characteristics after impact by high-energy quanta. At the same time, the noise measurements are important not only for estimating measurements of one of the key parameters

of the optoelectronic sensors — a photosignal/noise ratio. They are also substantially significant to clarify a nature of defects formed in the semiconductor structures exposed to penetrating radiation.

The present study provides and analyzes current-voltage characteristics (I-V curves), spectral photoelectric characteristics as well as values of electrical noises in the diodes and ATR sensors based on the p-InAsSbP/n-InAs/n-InAsSbP/n^+-InAs double heterostructures with a different size of the active areas, which were irradiated by γ-quanta from a ^{60}Co source with total irradiation doses within the range from 5 to $\sim 2 \cdot 10^3$ kGy.

1. Samples and research methods

The samples photoactive within the wavelengths $3.3-3.5\,\mu$m and similar to those described in the study [11] were based on three same-type double heterostructures p-InAs$_x$Sb$_{0.31(1-x)}$P$_{0.69(1-x)}$(Zn)(2–4 μm)/n-InAs(6–7 μm)/n-InAs$_x$Sb$_{0.31(1-x)}$P$_{0.69(1-x)}$(2–3 μm) grown during epitaxial processes #926, #1400 and #1698 on n^+-InAs tin-doped substrates (Sn, $n^+ = (2-3) \cdot 10^{18}\,\text{cm}^{-3}$), which were oriented in the plane (100) and had the thickness of $200\,\mu$m. The structures with the above-said compositions are often attributed to structures with II-type heterojunctions, in which quantum levels for charge carriers can be created in shallow quantum wells near the interfaces (see, for example, an energy band diagram and references in the study [3]). Recombination of the charge carriers at the said levels is significantly important only at the low temperatures, for example, at 4.2 K. In the present study, the selected interval of operating temperatures of the sensors was 200–300 K and, therefore, the said effects at the interface were excluded from consideration.

Methods of standard photolithography were used to form mesas of the height $5-10\,\mu$m with two following types on an epitaxial side of each DH, i.e. on the surface of p-InAsSbP:

a) shaped as a truncated pyramid with a base in the form of a non-symmetrical hexagon of the area of $3 \cdot 10^{-4}\,\text{cm}^2$, which are shown in Fig. 1, b and designated as #1400 in the subsequent figures;

b) shaped as disks of the diameter $Ø_m = 90$, 180, 190 and $280\,\mu$m (Fig. 1, c), which are hereinafter designated as #926 and #1698.

In the latter case, the surface of the round mesas included „wide" metal anodes, whose diameters $Ø_A$ were just a little (by $20-30\,\mu$m) inferior to the mesa diameters. Metal cathodes were outside the mesa as shown in Fig. 1, c and in our previous studies [11]). As in the most studies dedicated to the InAsSbP/InAs double heterostructures (see, for example, [24]), the cathodes were formed by sputtering in vacuum of Cr, Ni, Au with subsequent metal layer thickening by galvanic deposition of a golden film of the thickness of $2\,\mu$m. The anodes were made of an AgMn/Ni/Au composition. The present study has not applied special measures for protecting the mesa surface against environmental effects.

The metal cathode in the samples with the hexagonal mesas (Fig. 1, a, b) was shaped as a frame formed on a front face of the n^+-InAs substrate, while the very samples were manufactured as diode arrays mounted with a rear side of the n^+-InAs substrate with a transverse size 1×6.2 mm onto a non-conducting ceramic contact board of the thickness of 0.25 mm. As it is clear from Fig. 1, b, the transverse sizes of the trapeziodal anodes were significantly smaller than the mesa sizes and, therefore, made the major portion of the surface of the mesa/$p-n$-junction unshaded. These samples belong to a class of photodiode matrices with „surface illumination" (Front Surface Illuminated (FSI) PDs) and individual addressing to its elements; the matrix elements were connected to external devices by means of pairs of contacts C — A_i, where C — the cathode, A_i — the anode of the i-th element.

The diodes with the mesa diameter $Ø_m = 190\,\mu$m were mounted onto the waveguide/ATR crystal; the diodes and the waveguide were tightly connected („glued") using a transparent chalcogenide glass with refractive index $\tilde{n} = 2.4$, as proposed previously in the study [25] and shown in Fig. 1, d. The trapezoidal waveguide was produced by cleaving a polished GaAs plate (111) ($\tilde{n} = 3.5$) of the thickness of $250\,\mu$m; lengths of trapezoid sides (cleavage planes $\{110\}$) were 1.85 (side facets in Fig. 1, d), 3.3 (an upper facet for the analyte) and 5.15 mm (a lower facet for diode installation). The GaAs crystal was fixed on a metal holder using an epoxy glue VT-25-200 with boron nitride as a filler, which covered a part of one of the surfaces oriented in the plane $\{111\}$. As in the case of single diodes, operation of the two diodes ($D1$ and $D2$) in the ATR sensor was controlled via golden conductors connected to contact pads located on the side of the epitaxial layers.

The photodiodes used in the ATR sensor in Fig. 1, c are usually designated as Back-Side Illuminated (BSI) PDs. The said abbreviation will be used hereinafter in the graphs and the text to designate this PD type.

As in all the similar diodes (see, for example, [3,11]), electroluminescence (EL) spectra at 300 K had a maximum at the wavelength $\lambda_{\max} = 3.4-3.5\,\mu$m (300 K) and a FWHM of $0.4\,\mu$m. The photoresponse spectra in the BSI-type structures were similar to the EL spectra, but were shifted into a short-wave range by $\sim 0.1\,\mu$m in relation to the latter. In the spectrum maximum, photosensitivity of elements of the diode matrix was 1 A/W, wherein there was noticeable sensitivity at the short wavelengths ($\lambda < 3\,\mu$m) as well. The latter is caused by diffusion of photo-excited charge carriers from the surface of the p-InAsSbP absorbing layer to the $p-n$-junction (see, for example, [1]).

The diode pairs mounted to the GaAs crystal formed an optically-matched optopair „light-emitting diode–photodiode" due to the beams totally internally

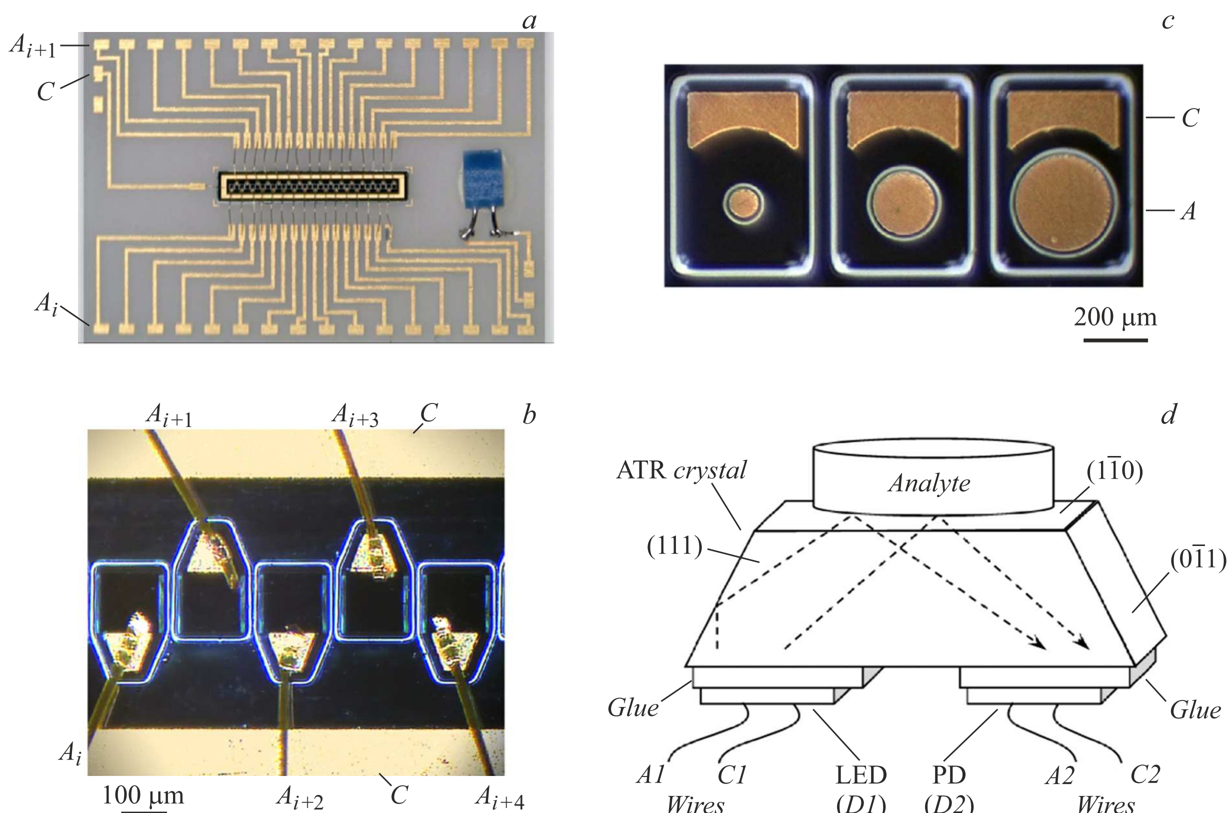

Figure 1. *a* — a general view of the matrix (diode array 1×32) mounted on a contact board, *b* — a photo of its fragment, which marks a common cathode (C), 5 mesas with golden wires (A_i) connected thereto; *c* — a photo of diodes with round mesas ($\varnothing_m = 90$, 180, 280 μm) and wide anodes (A); *d* — a schematic of the sensor with immersion coupling of the diodes and the ATR crystal, where „Glue" — an optical adhesive, „$D1, D2$" — diode chips, „Wires" — golden wires connected to the anodes (A) and the cathodes of the diodes (C), „*Analyte*" — an analyzed substance, the arrows — an approximate path of beams that are out of the light-emitting diode (LED, $D1$) and internally reflected at the ATR crystal/analyte interface and hit an absorbing layer of the photodiode (PD, $D2$). The schematic diagram is not in scale.

reflected from the GaAs/air interface (or the analyte[1]), which are conventionally showed by dashed arrows in Fig. 1, *d*. Due to design identity, the diodes $D1$ and $D2$ were interchangeable, i.e. they alternately acted as the LED and as the PD. Photocurrents I_{ph} in the PD were measured at constant forward LED bias without supplying bias to the PD, i.e. in a photovoltaic mode ($U = 0$, $I < 0$). In further discussion, the photocurrent will be understood as an absolute value of the PD photocurrent when $U = 0$, i.e. we will assume that $I_{\text{ph}} = |I| = \text{abs}(I)$.

Some samples with the round mesas (#926-11-...) were mounted with the substrate downwards to a nontransparent case TO-3 without a capability of further reliable measurement of their photovoltaic and optical properties. However, such a specific feature of mounting did not affect a capability of electrical measurements, including noise measurement.

The low-frequency noise was studied within the frequency range $1-10^3$ Hz at room temperature. The spectral noise density was measured in a circuit that consisted of a diode, a low-noise load resistance R_L and a power supply that were connected in series. The current fluctuations δI created by the forward-biased diode were transformed at the load resistance into voltage fluctuations $\delta U = \delta I \cdot R_L$ and supplied to a preamplifier 5113 EG&G and then to a spectrum analyzer Photon+. After subtraction of background noise, the current noise spectral density S_I was determined as $S_I = S_U \cdot [(R_L + R_0)/(R_L R_0)]^2$, where S_U is a voltage noise spectral density measured at the load resistance, R_0 is photodiode's zero bias resistance. The forward bias supplied to the diode was quite low so that differential resistance of the diode was always R_0.

The samples were irradiated by the ^{60}Co source at room temperature in a passive mode without supplying the bias to them. The diode matrix elements were exposed to γ-radiation only once, while all the other samples were multiply irradiated; in an initial state (before irradiation) the noise characteristics of the diodes were not significantly different from those published previously in the studies [2,10].

[1] With the analyte, it is more accurate to use the term „subjected to attenuated total reflection", since a portion of radiation is absorbed when it interacts with the analyte.

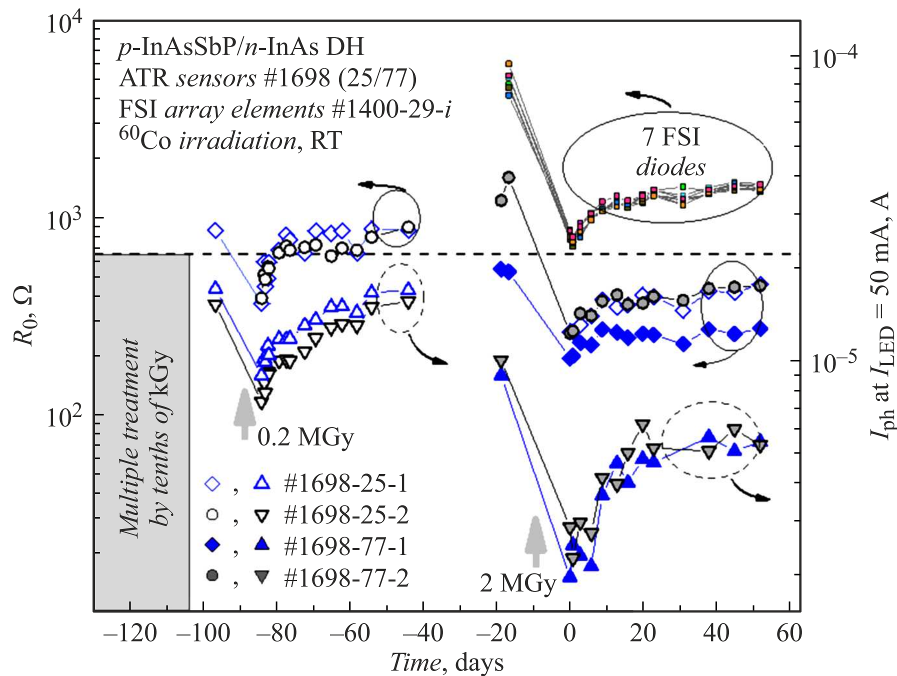

Figure 2. Dependence of the photocurrent I_{ph} of the optopairs „light-emitting diode−photodiode" at the LED current of 50 mA (the right scale) and of zero bias resistance R_0 of the two ATR sensors and the seven single FSI diodes (the left scale) on time after termination of irradiation with γ-quanta by the dose of 0.2 MGy ($t < -40$ days) and the dose of 2 MGy ($t > 0$).

2. Results of measurements and their discussion

2.1. Properties of the samples when the irradiation doses ≤ 60 kGy

At the first stage of the study, we measured the I-V and the noise characteristics of the FSI-diodes (300 K) based on the single p-InAsSbP/n-InAs/n^+-InAs heterostructures, which were similar to those described in the study [10] and irradiated with the ^{60}Co source with intensity of 288 rad/h. They were sequentially irradiated with the doses 11, 14 and 1150 Gy, thereby providing a final total irradiation dose of 1175 Gy. The selected irradiation doses did not provide any noticeable changes of the characteristics of the diodes, therefore, we do not provide them herein.

At the subsequent stages of the study, we used the ^{60}Co source with intensity ~ 1.1 Mrad/h and single diodes with the round mesas of the various diameter, including the diodes used in the ATR sensor and based on the InAsSbP/InAs double heterostructures, which were subsequently irradiated with the doses from 5 to 24 kGy. In all the measurements up to obtaining the total dose of 60 kGy, we neither detected any reliable features of variation of the I-V characteristics, the capacitance-voltage (C-V) and spectral characteristics and the photocurrents in the studied samples.

Further on, the samples were additionally irradiated with the doses 200 and 2000 kGy, thereby providing the total irradiation doses 260, 2000 and 2260 kGy for the various samples depending on their prehistory. Results of measurements of the characteristics of the so-irradiated samples are given below in Section 2.2 and 2.3.

It is quite obvious that along with the heterostructures, the passive elements included in the ATR sensor can also change their properties and affect operability of the sensor. In this regard, in addition to the diodes and the sensor, irradiation by γ-quanta was also delivered to materials and „reference" semiconductor plates used as included in the samples or having counterparts that are conveniently made for the measurements.

2.2. Electric and photoelectric properties

When the LED current increased from 10 to 100 mA (CW), the PD photocurrent I_{ph} in the ATR sensors monotonically increased from ~ 4 to $\sim 30\,\mu$A, which is close to the previously-obtained results for monolithic sensors based on the similar heterostructures [11]. When the sensors were exposed to γ-radiation of the dose of 200 kGy, I_{ph} temporarily decreased (Fig. 2). An increase of the irradiation dose to 2 MGy also resulted in degradation of I_{ph}, which tended to be restored in 30−40 days, as in the previous case. But at the large irradiation dose the value I_{ph} was not completely restored. Thus, for example, after $\sim 10^3$ hrs it was $\sim 60\,\%$ of the initial value (before irradiation) at the LED current of 50 mA and was not changed further on.

Among possible reasons of photocurrent reduction after irradiation with the ^{60}Co source, with a certain degree of caution one can name variation of optical transmittance

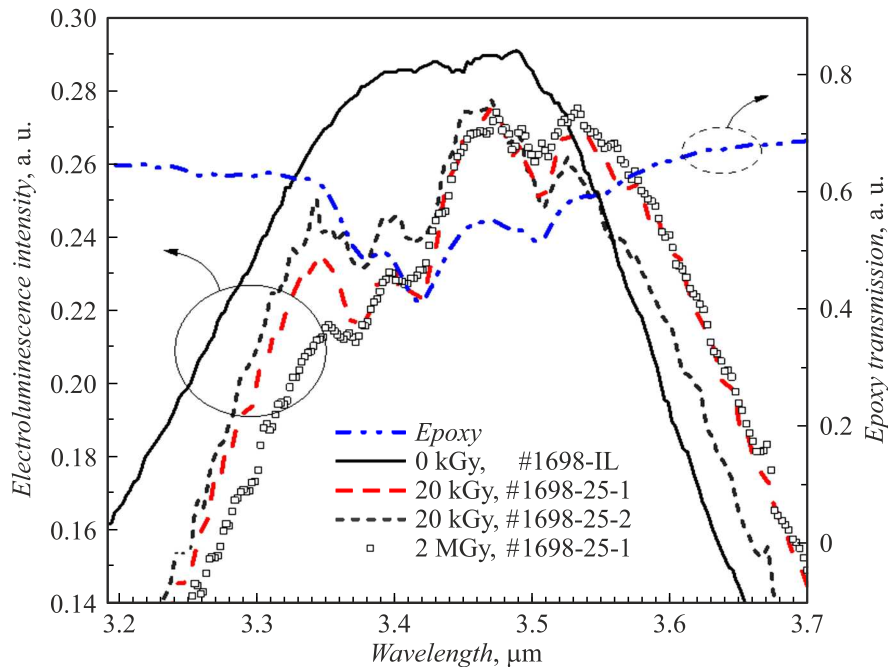

Figure 3. EL spectra near the peak for the initial diode structure (the black solid curve, the left scale), the spectra of the diodes in the sensor, which are irradiated with the doses 20, 2000 kGy (the black squares and the red discontinuous curve for the diode $D1$ and the dashed black curve for the diode $D2$, the left scale) and a transmittance spectrum of the glue VT-25-200 used for attaching the GaAs plate to the holder (the blue dash-dotted curve, the right scale).

of the n^+-InAs substrate, the GaAs crystal as well as the chalcogenide glass connecting them. However, the measurements on the reference samples made of the said materials did not identify significant changes of their optical properties, which would be enough for reduction of the above-mentioned photocurrent.

Another possible candidate responsible for reduction of I_{ph} and its subsequent restoration is a compound (epoxy) that connects the surface (111) of the GaAs crystal with the metal holder. Indeed, it is clear from Fig. 3 that unlike the initial LEDs the diodes included in the sensor had „irregular" EL spectra around the radiation maximum, while dips and peaks in the EL spectra completely corresponded to dips and peaks of the transmittance spectrum of the epoxy glue used during sensor installation, which is shown in the same figure. The said compliance can be easily related to absorption of a portion of LED radiation where the plane (111) of the ATR crystal is glued to the holder. At the same time, the epoxy glue that contacts the GaAs surface can be also considered as the analyte that interacts with the evanescent wave of LED radiation at the glue/GaAs interface. Thus, the data in Fig. 3 demonstrate that the sensor can measure the hydrocarbons with the absorption band near 3.4 μm similar to the evanescent wave sensors for gaseous and liquid hydrocarbons, which are described, for example, in the studies [26,27]. As can be seen from Fig. 3, distortions of the EL spectra before and after irradiation of the sensor, which are caused by absorption in the glue, are only slightly different from each other. Therefore, causes of variation/restoration of I_{ph} are first of all hidden in changes of properties of the active layers of the very diodes, rather than properties of the passive optical elements of the sensor or the n^+-InAs substrate.

Indeed, a property of spontaneous restoration of the electrical characteristics of the bulk n-InAs after termination of exposure to radiation was noted before as well (see, for example, the studies [21,28]). Therefore, the data for the samples irradiated with the dose of 0.2 MGy can be quite expected. At the same time, the above-said specific features of variation of I_{ph} in time were correlated to variation of the electrical parameters of the diodes. Thus, for example, the irradiated samples almost simultaneously retrieved both the initial value of zero bias resistance R_0 and the photocurrent value at 300 K. However, with the irradiation dose of 2 MGy (the right part in Fig. 2) the I-V characteristic parameters were not completely restored. At the same time, the I-V characteristic changes were especially noticeable in the diodes with the initially high values of R_0: among the diodes detailed in Fig. 2, it is first of all related to the FSI diodes included in the array, in which the value of R_0 decreased almost by an order after irradiation with the dose of 2 MGy.

The above-said patterns of variation of the electrical properties during irradiation were generally repeated for the I-V characteristics at the decreased temperatures as well. At the same time, at the high currents the diode I-V characteristics before irradiation and after it were digestibly described by a function of the kind $I = I_0[\exp(qU/\beta kT) - 1]$, where U is a bias voltage, q is the charge of the electron, k is

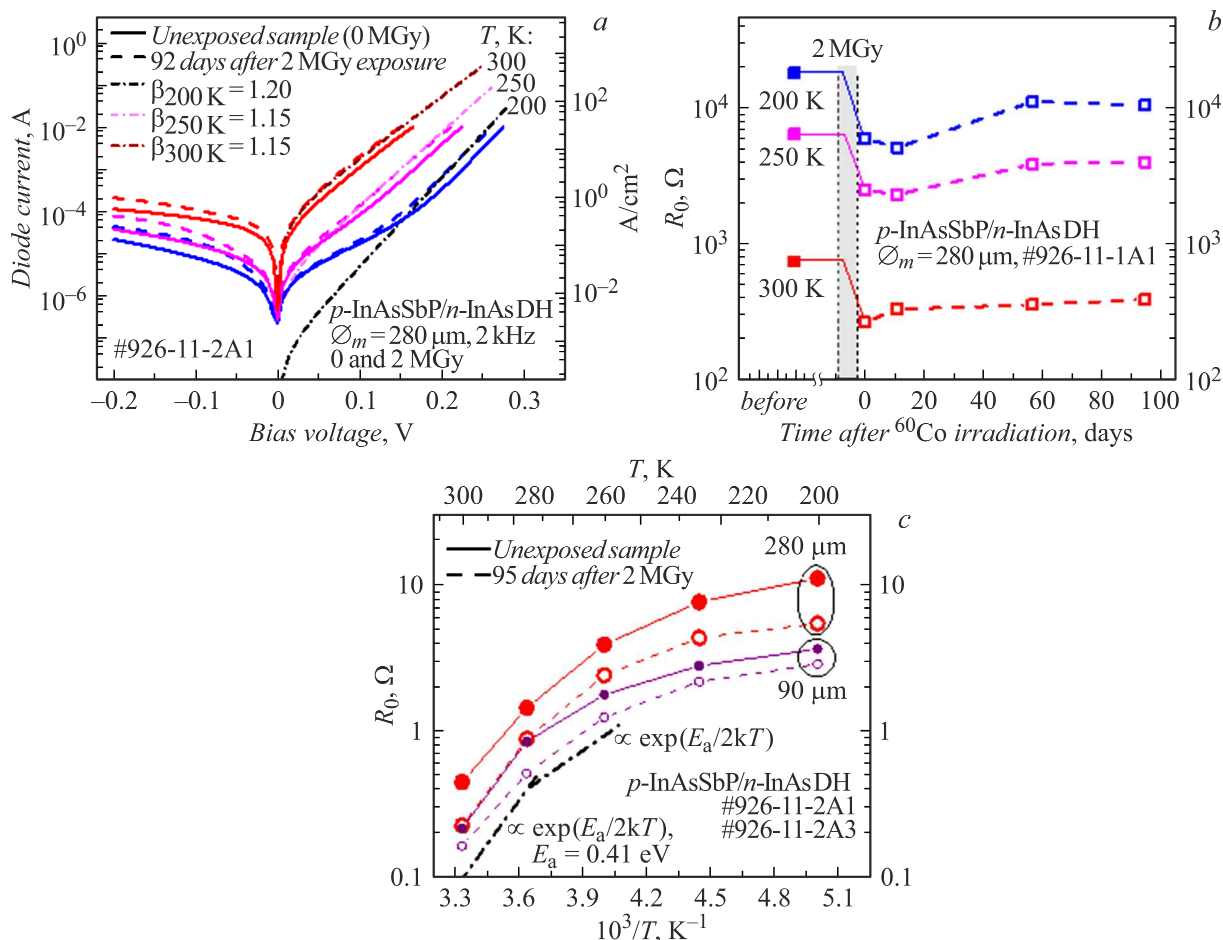

Figure 4. Electrical characteristics of the diodes with the round mesa $\varnothing_m = 280$ and $90\,\mu$m at the temperatures 200−300 K before and after termination of irradiation with the dose of 2 MGy (^{60}Co): *a* — the I-V characteristics, *b* — zero bias resistance R_0 and *c* — R_0A, where *A* — the areas of the mesa surface: the solid lines and the filled symbols — the unexposed samples, the dashed lines and the unfilled („empty") symbols — the irradiated samples, the dash-dotted lines in Fig. (*a, c*) —the values obtained from the modified Shockley formula with the parameter β being equal to 1.15 (300 K), 1.15 (250 K) and 1.2 (200 K). The data are provided for two groups of the same-type samples, therefore, numerical values are not necessarily coincident when transiting from one figure to another.

the Boltzmann constant, T is a temperature, $(-I_0)$ is a saturation current and β is an I-V characteristic ideality factor (the dash-dotted curves in Fig. 4, *a*). The ideality factor β insignificantly increased with a decrease of the temperature, obviously reflecting an increase of a contribution by a generation-recombination current to the total diode current. At the low temperatures, regions of the small biases ($U < 0.15$ V) distinctly exhibited current leakages related to tunneling of the charge carriers through a potential barrier, which is a typical property of such diodes [2,29]. As it is clear from Fig. 4, *a*, the effect of radiation with γ-quanta was mainly reduced to an increase of the currents (for example, to the increase of the value of I_0) while preserving a general kind of the I-V characteristic, i.e. while preserving the values of β. At the same time, the I-V characteristic changes related to irradiation were more noticeable in an reverse branch than for a forward branch.

A „fast" phase of partial restoration of the values of R_0 for all the measurement temperatures was ended in 30−40 days after termination of radiation with the dose of 2 MGy (Fig. 4, *b*). Approximately the same value of the time of termination of the „fast" phase of restoration of R_0 and I_{ph} was observed for small irradiation doses detailed in Fig. 2.

The kind of the dependence of the product R_0A on the reciprocal temperature in Fig. 4, *c* at the temperatures 280−300 K was typical for the diodes with a diffusion mechanism of current passage, since the condition $R_0A \propto \exp(E_a/kT)$ ($E_g \approx E_a = 0.41$ eV) was fulfilled. And at $T = 200-250$ K the temperature change of R_0A was smoother than for the diodes with the current is determined by recombination in a space charge region ($R_0A \propto \exp(E_a/2kT)$).

2.3. Low-frequency noises

Fig. 5, *a* shows the values of noises ($f = 10$ Hz, 300 K) and resistances R_0 at the various times before and after

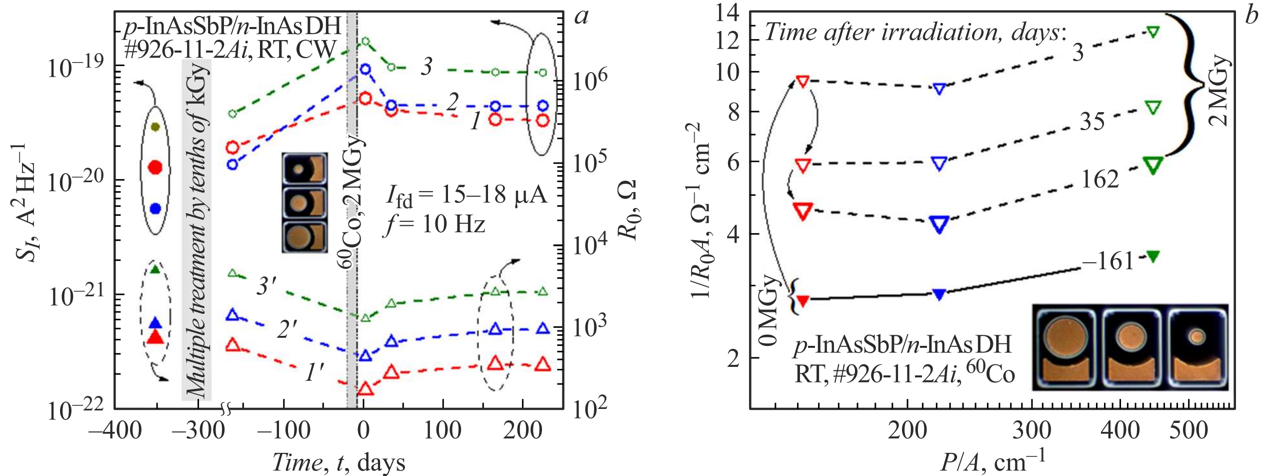

Figure 5. *a* — the dependence of the noise $(S_I)_{10\,\mathrm{Hz}}$ and resistance (R_0) on time to be passed after termination of irradiation for the three BSI diodes with the mesa diameters 280, 180 and 90 μm (the curves *1*(*1′*), *2*(*2′*) and *3*(*3′*), respectively), *b* — the dependence of the product R_0A (300 K) on a ratio of the perimeter (P) and the diodes area (A) before and after irradiation with the dose of 2 MGy at the various times.

irradiation with the dose of 2 MGy in the three diodes with the mesa diameters 90, 180 and 280 μm. It is clear from Fig. 5, *a* that irradiation results in the increase of the noises in several times, wherein over time the noise level as well as the values of resistances R_0 tend to be restored to the previous values. These metamorphoses are usually related to healing (or annihilation) of defects introduced when the crystal was exposed to radiation. With great probability, in our case such defects were mainly formed on the mesa surface to create a leakage conducting channel thereon. It is indicated, in particular, by a dependence of a reciprocal value of the product R_0A on a mesa perimeter/area ratio P/A in Fig. 5, *b*, whence it follows that the electrical parameters of the diodes with the high ratio P/A turned out to be the most sensitive to exposure to γ-quanta and the relative contribution by the surface currents in them is the largest. For some diodes based on the semiconductors, including the compounds $A^{III}B^{V}$ and $A^{II}B^{VI}$, excessive noises in the form of noise $1/f$ are exactly induced by the leakage current along a surface/slope of the mesa structure [30–32]. Therefore, the authors are inclined to think that the observed noise is attributed to a current flowing along a side surface of the mesa structure. In our opinion, this assumption is confirmed by the data in Fig. 6, *a*. They show that noises that are supposedly of a generation-recombination nature ($S_I \propto I$) and normalized to the mesa perimeter (the dimension [$A^2Hz^{-1}cm^{-1}$]) are linearized in the coordinates ($S_I/\pi\O_m$) vs (I/A) with a unified coefficient of proportionality for the samples with the various mesa diameters.

According to theoretical representations [33], in combination with a frequency dependence of the kind $S_I \propto 1/f$ (Fig. 7) dependences of the kind $S_I \propto I$ (Fig. 6, the curve *2*) reflect that the noise is formed with involvement of closely located defects („fluctuators"), which can be donor-acceptor pairs, at the diode periphery. In 35 days after irradiation the kind of the dependence $S_I(I)$ (Fig. 6, *b*, the curve *3*) somewhat changed. The kind of this dependence still indicate prevalence of the recombination processes with involvement of the closely located defects. After 35 days the noise was almost the same and was still different from the initial one (the curves *4, 5* in Fig. 6, *b*). In turn, the initial dependence $S_I(I)$ for the unexposed sample (Fig. 6, *b*, the curve *1*) is obviously a superposition of the quadratic function of the kind $S_I \propto I^2$, which reflects the recombination processes with involvement of single Shockley-Read-Hall defects and a linear function of the kind $S_I \propto I$, which is typical for describing the properties of the closely located defects. Thus, before irradiation with γ-rays the noise is formed with involvement of two types of defects that are located both within a semiconductor volume [15,16,21,22] and on the diode periphery, including the interface between the DH layers. The initial period after irradiation exhibits defects of one prevalent type only.

Over time, the surface component of the current of the irradiated diodes decreased (R_0 was increasing) and the dependence S_I on (I) (Fig. 6, *b*, the curve *4*) was determined by a superposition of the linear and quadratic dependences and was different from the initial one (Fig. 6, *b*, the curve *1*) by increased values of the noises and the large contribution by the linear dependence S_I on the current. Thus, it can be assumed that predominantly the closely located defects are gradually healed (annihilated). At the same time, within the entire frequency range the frequency dependence of the noise still kept the kind $1/f$ for the entire period passed after irradiation of the samples (Fig. 7). With rare exceptions [29], this kind of the frequency dependence is typical for most InAs-based diodes as well as for many other semiconductors.

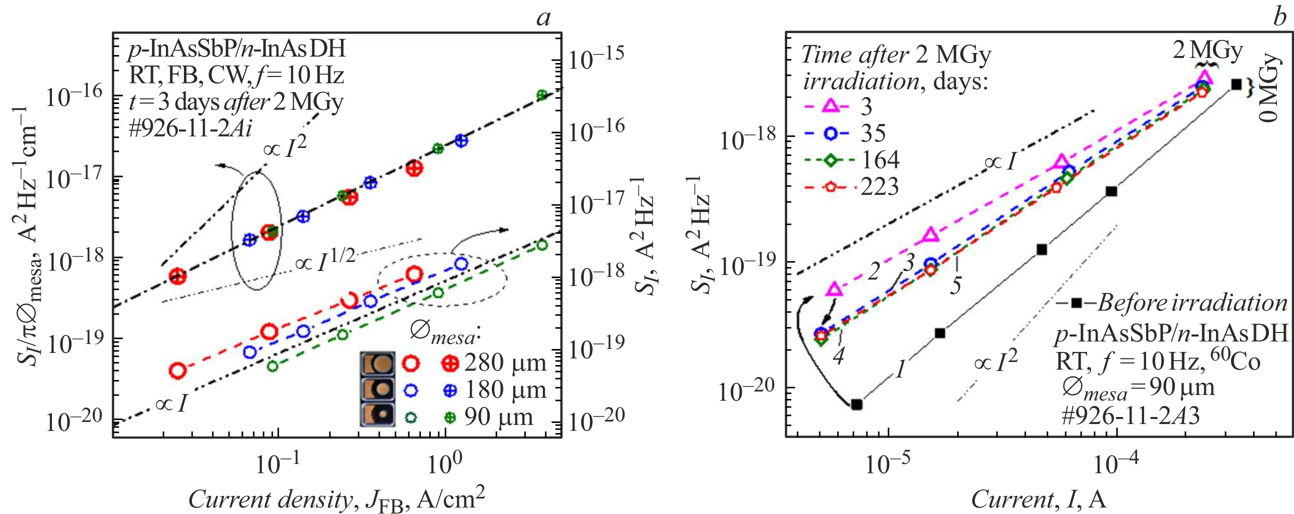

Figure 6. *a* — the dependence of the noise S_I (the right scale) and the perimeter-normalized noise $S_I/\pi\O_m$ (the left scale) on the forward current density in the diodes with $\O_m = 90$, 180 and 280 μm in three days after termination of irradiation with the dose of 2 MGy; *b* — the dependence of the noise on the forward current in the sample $\O_m = 90\,\mu$m before (the solid symbols, the curve *1*) and after irradiation (the „empty" symbols) in 3, 35, 164 and 223 days (the curves *2–5*, respectively) after its termination at the temperature of 25 °C–29 °C.

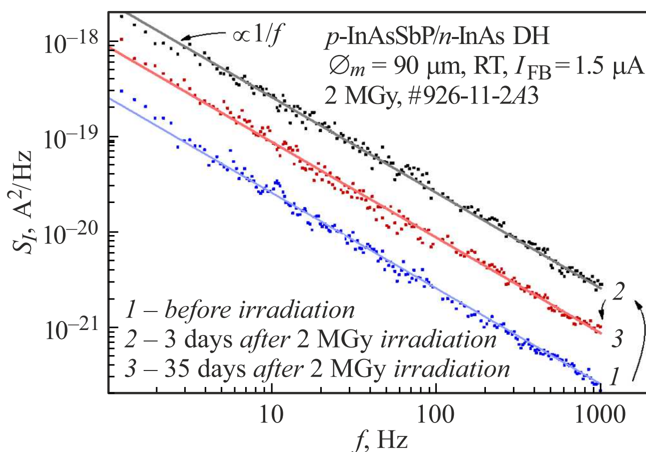

Figure 7. Frequency dependence of the current noise S_I for the diode $\O_m = 90\,\mu$m: *1* — before irradiation, *2* — in three days after irradiation with the dose of 2 MGy, *3* — in 35 days after termination of irradiation. The straight lines mean values of the functions of the kind $S_I \propto 1/f$.

Conclusions

Thus, the *p*-InAsSbP/*n*-InAs diode structures with the mesa diameters from 90 to 280 μm and the optoelectronic ATR sensors based thereon are stable to exposure to γ-radiation by ^{60}Co at the irradiation doses below ~ 0.1 MGy, i.e. they keep almost unchanged parameters, such as the low-frequency noise level S_I measured for the forward current as well as zero bias resistance R_0 and the photocurrent I_{ph}. At the average irradiation doses (~ 0.2 MGy), the said parameters degrade in time and in a month they are spontaneously restored to the previous values. After the large irradiation doses (2 MGy), there is also a degradation of the parameters (double to triple reduction of R_0, I_{ph}, the increase of the noises S_I) and a phase of partial restoration of their previous values. At the same time, upon termination of this phase we detect that the parameters of the diodes and the ATR sensor are irreversibly degraded when they are irradiated by the ^{60}Co source. The said changes are mainly caused by formation and partial healing (annihilation) of the defects of the two types, which are formed within the volume of the heterostructures and near the surface thereof. It is most likely that the latter belong to a class of the closely located defects, but answering an issue of their nature requires additional research.

Acknowledgments

The authors would like to thank N.D. Il'inskaya, A.A. Usikova and A.A. Lavrov for their assistance in the study. Execution of the studies was initiated by a start of work for the project of the program HORIZON 2020 (project „Embedded Electronic Solutions for Polymer Innovative Scanning Methods using Light Emitting Devices for Diagnostic Routines"(„El Peacetolero", Grant Agreement ID:945320)).

Conflict of interest

The authors declare that they have no conflict of interest.

References

[1] H. Lin, Z. Zhou, H. Xie, Y. Sun, X. Chen, J. Hao, S. Hu, N. Dai. Phys. Status Solidi A, **218**, 2100281 (2021). DOI: 10.1002/pssa.202100281N

[2] N. Dyakonova, S.A. Karandashev, M.E. Levinshtein, B.A. Matveev, M.A. Remennyi. Infrared Phys. Technol., **111**, 103460 (2020). DOI: 10.1016/j.infrared.2020.103460

[3] S.A. Karandashev, B.A. Matveev, and M.A. Remennyi. Semiconductors, **53** (2), 147 (2019). DOI: 10.1134/S1063782619020131

[4] A. Krier, M. Yin, A.R.J. Marshall, S.E. Krier. J. Electron. Mater., **45**, 2826 (2016). DOI: 10.1007/s11664-016-4373-0

[5] G.P. Forcade, C.E. Valdivia, S. Molesky, S. Lu, A.W. Rodriguez, J.J. Krich, R. St-Gelais, K. Hinzer. Appl. Phys. Lett., **121**, 193903 (2022). DOI: 10.1063/5.0116806

[6] A.V. Zagnit'ko, I.D. Matsukov, V.V. Pimenov, S.E. Sal'nikov, D.Yu. Fedin, V.I. Alekseev, S.M. Vel'makin. Technical Physics, 67 (6), 664 (2022). DOI: 10.21883/JTF.2022.06.52505.325-21

[7] Y. Wang, A. Shi, X. Wang, J. Bai, L. Wang, F. Li. Infrared Phys. Technol., **108**, 103335 (2020). DOI: 10.1016/j.infrared.2020.103335

[8] M. Köhring, S. Böttger, U. Willer, W. Schade. Sensors, **15**, 12092 (2015). DOI: 10.3390/s150512092 PMCID: PMC4481913

[9] G.Yu. Sotnikova, S.A. Aleksandrov, G.A. Gavrilov. UPF, (in Russian). **10** (4), 389 (2022). DOI: 10.51368/2307-4469-2022-10-4-389-403

[10] M.E. Levinshtein, B.A. Matveev, N. Dyakonova, Technical Physics Letters, **49** (6), 16 (2023). DOI: 10.21883/PJTF.2023.11.55533.19524

[11] S.A. Karandashev, T.S. Lukhmyrina, B.A. Matveev, M.A. Remennyy, A.A. Usikova. Phys. Status Solidi A, **219** (2), 2100456 (2022). DOI: 10.1002/pssa.202100456

[12] M. Broudin, M.B. Chouikha. EPJ Nucl. Sci. Technol., **8**, 22 (2022). DOI: 10.1051/epjn/2022013

[13] M.I. Boussandel, A. Fathallah, J.-M. Armani, F. Armi, G. Klisnick, Z. Ren, M.B. Chouikha. In 2023 *RADECS Data Workshop* (IEEE, France, 2023), p. 1–5. DOI: 10.1109/RADECS59798.2023.10752868

[14] P.P. Trokhimchuck. Proceedings of the 12 International Conf. „Interaction of Radiation with Solids", Minsk, 19–22 September 2017, 193 (2017).

[15] V.N. Brudnyi, N.G. Kolin, A.I. Potapov, Semiconductors, 37(4), 390 (2003). DOI: 10.1134/1.1568456

[16] N.V. Zotova, S.A. Karandashev, B.A. Matveev, M.A. Remennyi, N.M. Stus', N.A. Voronova, G.M. Gusinskii, V.O. Naydenov. Technical Physics Letters, **30** (1), 35 (2004). DOI: 10.1134/1.1646703

[17] V.V. Mikhailovskii, V.I. Sugakov, O.N. Shevtsova, P.G. Litovchenko, A.Ya. Karpenko, G.A. Vikhlii. Voprosy atomnoi nauki i tekhniki. Seriya: Fizika radiatsionnykh povrezhdenii i radiatsionnoe materialovedenie, **55** (2), 90 (2007) (in Russian).

[18] G.R. Savich, D.E. Sidor, X. Du, M. Jain, C.P. Morath, V.M. Cowan, J.K. Kim, J.F. Klem, D. Leonhardt, S.D. Hawkins, T.R. Fortune, A. Tauke-Pedretti, G.W. Wicks. Proc. SPIE 9070, Infrared Technology and Applications XL, 907011 (24 June 2014). DOI: 10.1117/12.2050535

[19] G.R. Savich. *Analysis and Suppression of Dark Currents in Mid-Wave Infrared Photodetectors* (University of Rochester, NY., 2015)

[20] I. Bolshakova, S. Belyaev, M. Bulavin, V. Brudnyi, V. Chekanov, V. Coccorese, I. Duran, S. Gerasimov, R. Holyaka, N. Kargin, R. Konopleva, Ya. Kost, T. Kuech, S. Kulikov, O. Makido, Ph. Moreau, A. Murari, A. Quercia, F. Shurygin, M. Strikhanov, S. Timoshyn, I. Vasil'evskii, A. Vinichenko. Nucl. Fusion, **55**, 083006 (2015). DOI: 10.1088/0029-5515/55/8/083006

[21] N. Kekelidze, B. Kvirkvelia, E. Khutsishvili, T. Qamushadze, D. Kekelidze, R. Kobaidze, Z. Chubinishvili, N. Qobulashvili, G. Kekelidze. World Acad. Sci. Eng. Technol. Int. J. Phys. Math. Sci., **13**, 13 (2019).

[22] V.N. Brudnyi, S.N. Grinyaev, N.G. Kolin. Semiconductors, **39** (4), 385 (2005). DOI: 10.1134/1.1900249

[23] A.N. Klochkov, A.N. Vinichenko, A.A. Samolyga, S.M. Ryndya, M.V. Poliakov, N.I. Kargin, I.S. Vasil'evskii. Appl. Surf. Sci., **619**, 156722 (2023). DOI: 10.1016/j.apsusc.2023.156722

[24] A.A. Pivovarova, N.D. Il'inskaya, E.V. Kunitsyna, Yu.P. Yakovlev. Semiconductors, 57 (8), 685-690 (2023). DOI: 10.61011/SC.2023.08.57626.5391 DOI: 10.61011/FTP.2023.08.56972.5391

[25] S.A. Karandashev, B.A. Matveev, M.A. Remennyi, Mohamed Ben Chouikha. Patent RF 2753854 (2021) (in Russian).

[26] S. McCabe, B. MacCraith. Electron. Lett., **29** (19), 1719 (1993). DOI: 10.1049/el:19931143

[27] B.A. Matveev, N.V. Zotova, S.A. Karandashev, M.A. Remennyi, N.M. Stus, G.N. Talalakin. In Proc. CAOL2003 1st Int. Conf. Adv. Optoelectron. Lasers Jontly 1st Workshop Precis. Oscil. Electron. Opt. IEEE Cat No 03EX715 (IEEE, 2003), p. 138–140. DOI: 10.1109/CAOL.2003.1251237

[28] S.K. Nikogosyan, V.A. Saakyan. Preprint EFI, H-845 (72)-85 (Yerevan Physics Institute, Yerevan, 1985) (in Russian).

[29] A. Tkachuk, V. Tetyorkin, A. Sukach. In 2021 Int. Semicond. Conf. CAS (IEEE, 2021), p. 279–282. DOI: 10.1109/CAS52836.2021.9604182

[30] A. Van der Ziel. Physica, **48** (2), 242 (1970). DOI: 10.1016/0031-8914(70)90025-X

[31] A. Soibel, D.Z.-Y. Ting, C.J. Hill, M. Lee, J. Nguyen, S.A. Keo, J.M. Mumolo, S.D. Gunapala. Appl. Phys. Lett., **96**, 111102 (2010). DOI: 10.1063/1.3357429

[32] T. Tansel, K. Kutluer, A. Muti, Ö. Salihoglu, A. Aydinli, R. Turan. Appl. Phys. Express, **6**, 032202 (2013). DOI: 10.7567/APEX.6.032202

[33] G.P. Zhigal'skii. *Fluktuatsii i shumy v elektronnykh tverdotel'nykh priborakh* (Fizmatlit, M., 2012), s. 512 (in Russian).

Translated by M.Shevelev